electronics

Article

A Single-Stage LED Streetlight Driver with Soft-Switching and Interleaved PFC Features

Chun-An Cheng, Chien-Hsuan Chang, Hung-Liang Cheng, En-Chih Chang *, Tsung-Yuan Chung and Man-Tang Chang

Department of Electrical Engineering, I-Shou University, Dashu District, Kaohsiung City 84001, Taiwan
* Correspondence: enchihchang@isu.edu.tw; Tel.: +886-7-657-7711 (ext. 6642)

Received: 10 July 2019; Accepted: 15 August 2019; Published: 18 August 2019

Abstract: This paper presents a single-stage driver with soft-switching and interleaved power-factor correction (PFC) features suitable for light-emitting diode (LED) energy-saving streetlight applications. The proposed LED streetlight driver integrates an interleaved buck-boost PFC converter with coupled inductors and a half-bridge LLC resonant converter into a single-stage power-conversion circuit with reduced voltage stress on the DC-linked capacitor and power switches, and it is suitable for operating at high utility-line voltages. Furthermore, coupled inductors in the interleaved buck-boost PFC converter are operated in discontinuous-conduction mode (DCM) for accomplishing PFC, and the half-bridge LLC resonant converter features zero-voltage switching (ZVS) to reduce switching losses of power switches, and zero-current switching (ZCS) to decrease conduction losses of power diodes. Operational modes and design considerations for the proposed LED streetlight driver are introduced. Finally, a 144 W (36V/4A)-rated LED prototype driver is successfully developed and implemented for supplying a streetlight module and operating with a utility-line input voltage of 220 V. High power factor, low output-voltage ripple factor, low output-current ripple factor, and high efficiency are achieved in the proposed LED streetlight driver.

Keywords: converter; LED; power-factor correction (PFC); soft-switching; streetlight driver

1. Introduction

With recent developments in green lighting and energy saving around the world, light-emitting diodes (LEDs) are characterized by their small size, long life, high brightness and environmental friendliness [1–3]. As a result, LEDs have begun to play important roles as new solid-state light sources for indoor and outdoor energy-saving applications in our daily lives [4–11].

Streetlights that illuminate the road are designed to provide a safe night-time environment for cars, motorcycles, cyclists and pedestrians. The traditional source of illumination for streetlight applications is high-pressure mercury lamps, because of their low installation cost. However, high-pressure mercury lamps consume more energy and save less electricity. In addition, the discharge tubes of these lamps contain mercury vapor, which is harmful and can cause pollution to our environment when the lamp is exhausted. Therefore, LED streetlights with energy-saving features have begun replacing traditional high-pressure mercury street lamps [12,13]. Traditional two-stage drivers for LED streetlight applications include AC–DC converters with power-factor correction (PFC) and DC–DC converters that provide rated voltage and current to the LED streetlight [14,15]. However, the circuit is not efficient, and requires more power switches and components in a conventional two-stage streetlight driver. The literature presents some single-stage streetlight drivers that integrate an AC–DC converter with a DC–DC converter [16–20]. Figure 1 shows an existing single-stage LED streetlight driver, which combines an interleaved boost converter with a half-bridge-type LLC resonant converter into a single-stage power converter for supplying the LED street-lighting module at a utility-line voltage of 110V [16]. The LED streetlight driver comprises a low-pass filter, a bridge rectifier (D_{r1}, D_{r2}, D_{r3} and D_{r4}), two capacitors (C_{in1} and C_{in2}), two diodes (D_{B1} and D_{B2}), two inductors (L_1 and L_2), two power switches (S_1 and S_2), a DC-linked capacitor C_{DC}, a resonant capacitor C_r and an inductor L_r, a center-tapped transformer T with two output windings, two diodes (D_1 and D_2), a capacitor C_o and the LED streetlight module. This kind of single-stage streetlight driver based on interleaved boost conversion is suitable for operating at utility-line voltages from 100~120 V in American and Asian countries, but will tolerate high voltage levels on the DC-linked capacitor C_{DC} when it operates at higher utility-line voltages due to boost-type power conversion, such as the 220~240 V in European countries. In addition, the voltage stresses of the power switches in this version will increase. Another existing single-stage LED streetlight driver, which integrates an interleaved boost PFC converter with a half-bridge-type series-resonant converter cascaded with a bridge rectifier for supplying the LED street-lighting module at a utility-line voltage of 220 V was proposed in [20], and high voltage stresses of power switches occurred in this version due to the boost-type power conversion; therefore, the level of DC-bus voltage is increased, and two DC-linked capacitors are required.

To meet these challenges, this paper proposes and implements a single-stage LED streetlight driver based on interleaved buck-boost conversion with PFC and soft-switching functions, which is suitable for operating at high utility-line voltages along with reduced voltage levels on the DC-linked capacitor and decreased voltage stresses on the power switches due to a buck-boost-type power conversion. This paper introduces the description and analysis of the operating modes, the design considerations of the key circuit components in the proposed LED streetlight driver, and experimental results obtained from the 144 W (36V/4A)-rated prototype circuit are included.

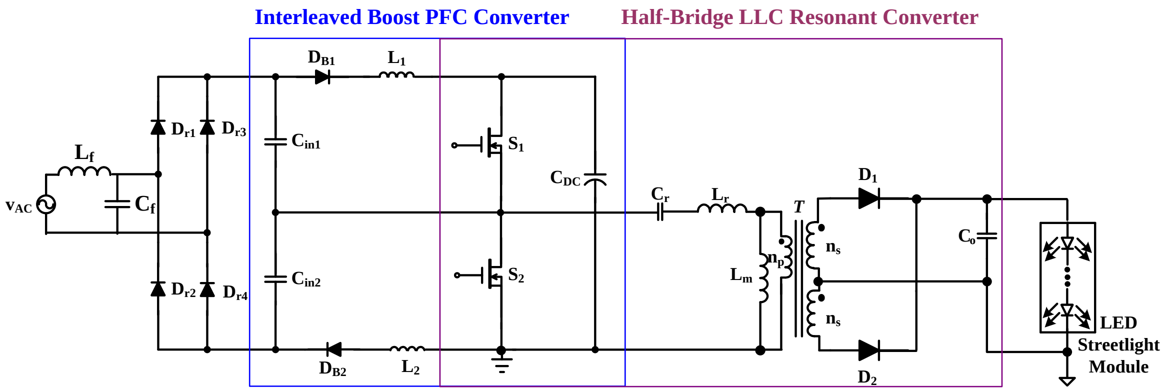

Figure 1. The existing single-stage LED streetlight driver.

2. Circuit Derivation and Analysis of the Proposed Single-Stage LED Streetlight Driver

Figure 2a shows the original two-stage LED streetlight driver, which consists of buck-boost PFC converter #1 and buck-boost PFC converter #2 with interleaved operation in series connection with a half-bridge LLC resonant converter. In addition, the two coupled inductors are employed instead of single-winding inductors in order to accomplish buck-boost conversion. Figure 2b shows the presented LED streetlight driver with soft-switching and interleaved PFC feature, which integrates an interleaved buck-boost PFC converter with a half-bridge LLC resonant converter into single-stage power conversion and includes a low-pass filter (L_f and C_f), a bridge rectifier (D_{r1}, D_{r2}, D_{r3} and D_{r4}), two capacitors (C_{in1} and C_{in2}), two coupled inductors (L_{B1} and L_{B2}; L_{B3} and L_{B4}), four diodes (D_{B1}, D_{B2}, D_{B3}, and D_{B4}), two power switches (S_1 and S_2), a DC-bus capacitor (C_{DC}), a resonant capacitor (C_r), a resonant inductor (L_r), a center-tapped transformer T with a magnetizing inductor L_m and two output windings, two output diodes D_1 and D_2, an output capacitor (C_o) and the LED streetlight module. In addition, the diodes D_{B2} and D_{B3} are used to prevent current from entering the inductors L_{B2} and L_{B3} from the AC mains voltage sources. Furthermore, diodes D_{B1} and D_{B4} are capable of preventing the inductor currents from returning to the input capacitors C_{in1} and C_{in2}. Since the voltage on the capacitor C_{in1} or C_{in2} is half of the utility-line voltage, the DC-bus voltage and the peak current of each coupled inductor will also be half. Due to the reduced DC-bus voltage, power switches with decreased voltage-stress can be utilized in the proposed LED streetlight driver, which is advantageous for high utility-line voltage applications.

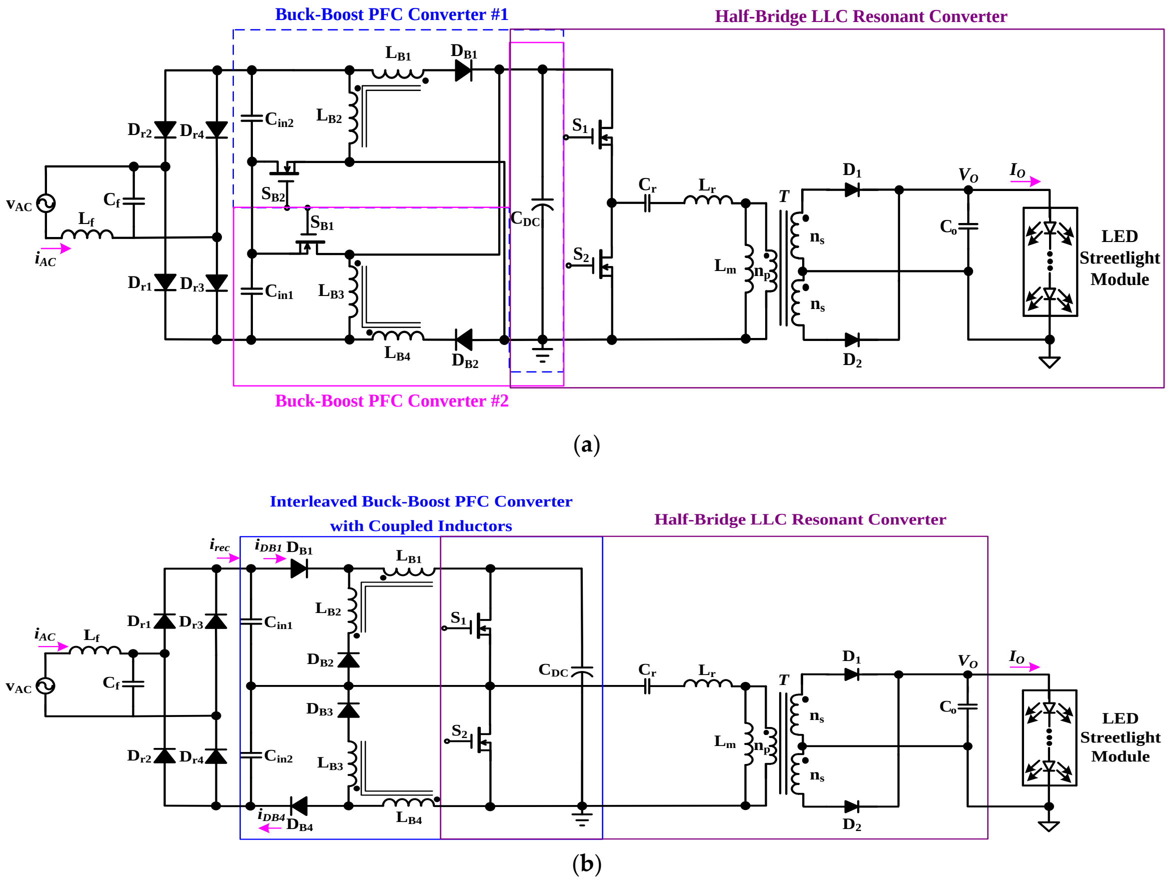

Figure 2. (**a**) Original two-stage LED streetlight driver; (**b**) the presented single-stage LED streetlight driver with coupled inductors and interleaved PFC feature.

Figure 3 shows a simplified circuit of the proposed single-stage LED streetlight driver when analyzing its operating modes. To describe the operation of the proposed LED streetlight driver, the following assumptions are made.

(a) Since the switching frequency of the power switches is much higher than the utility-line frequency, the sinusoidal utility-line voltage can be considered to be a constant value in each high-frequency switching period.
(b) The voltage sources V_{REC1} and V_{REC2} of capacitors C_{in1} and C_{in2}, respectively, represent the rectified input utility-line voltages.
(c) The power switches S_1 and S_2 operate complementarily, and their intrinsic body diode and drain-source capacitance are taken into consideration.
(d) The turn-on voltage drops of diodes (D_{B1}, D_{B2}, D_{B3}, D_{B4}, D_1 and D_2) are omitted.
(e) To naturally obtain PFC, the coupled inductors (L_{B1} and L_{B2}; L_{B3} and L_{B4}) are designed to operate in discontinuous-conduction mode (DCM).

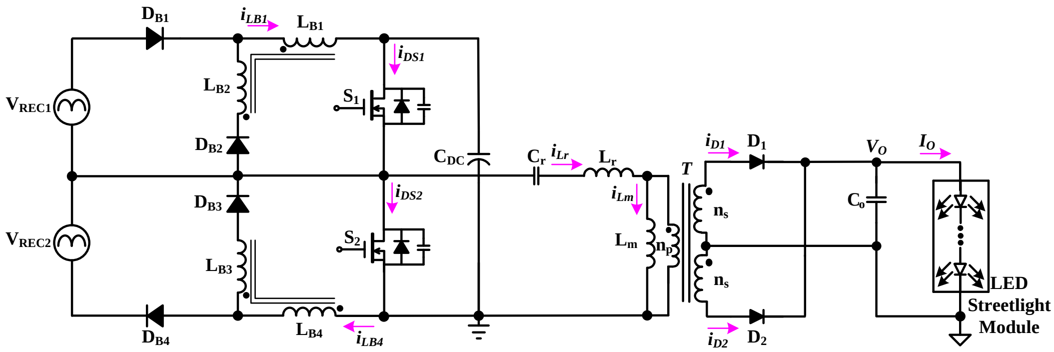

Figure 3. The simplified circuit of the presented single-stage LED driver for streetlight applications.

The operational modes and key waveforms of the LED streetlight driver proposed in this paper are shown in Figures 4 and 5, respectively, and the analysis of the operation is described in detail below.

Mode 1 ($t_0 \le t < t_1$; in Figure 4a): When the switch voltage v_{DS1} decreases to zero and the body diode of switch S_1 is forward-biased at time interval t_0, this mode begins and the power switch S_1 turns on with zero-voltage switching (ZVS). The voltage source V_{REC1} charges the coupled inductor L_{B1} through diode D_{B1} and switch S_1. The inductor current i_{LB1} increases linearly from zero and can be given by:

$$i_{LB1}(t) = \frac{\left|\sqrt{2}v_{AC-rms}\sin(2\pi f_{AC}t)\right|}{2L_{B1}}(t-t_0) \tag{1}$$

where $v_{AC\text{-}rms}$ represents the rms value of input utility-line voltage, and f_{AC} represents the utility-line frequency.

The resonant inductor L_r and magnetizing inductor L_m provide energy to the resonant capacitor C_r and to DC-linked capacitor C_{DC} through the body diode of switch S_1, and to the output capacitor C_o and the LED streetlight module through transformer T and output diode D_1. The diode D_{B3} is forward-biased, and the coupled inductors L_{B3} and L_{B4} provide energy to the drain-source capacitor of switch S_2 through diode D_{B3}. This mode ends when the resonant inductor current i_{Lr} is zero at time t_1.

Mode 2 ($t_1 \le t < t_2$; in Figure 4b): This mode is activated when the resonant inductor current i_{Lr} reaches zero at t_1. The voltage source V_{REC1} continues charging the coupled inductor L_{B1} through diode D_{B1} and switch S_1.

The capacitors C_{DC}, the magnetizing inductor L_m and the coupled inductors L_{B3} and L_{B4} provide energy to the drain-source capacitor of switch S_2, the resonant inductor L_r and the resonant capacitor C_r through D_{B3}, and to the output capacitor C_o and the LED streetlight module through transformer T and output diode D_1. When the magnetizing inductor current i_{Lm} and inductor current i_{LB4} become zero at t_2, this mode finishes.

Mode 3 ($t_2 \le t < t_3$; in Figure 4c): At t_2, the voltage source V_{REC1} continues charging the coupled inductor L_{B1} through D_{B1} and S_1. The capacitors C_{DC} provides energy to the resonant inductor L_r, the resonant capacitor C_r, and the magnetizing inductor L_m through S_1, and to the output capacitor C_o and the LED streetlight module through transformer T and output diode D_1. This mode ends when the diode current i_{D1} becomes zero at t_3.

Mode 4 ($t_3 \le t < t_4$; in Figure 4d): This mode activates when i_{D1} is zero at t_3. The voltage source V_{REC1} continues charging the coupled inductor L_{B1} through D_{B1} and S_1. The capacitor C_{DC} continues providing energy to the inductors L_r and L_m and to C_r through S_1. The output capacitor C_o provides energy to the LED streetlight module. The coupled-inductor current i_{LB1} reaches its peak value at t_4, which is denoted as $i_{LB1\text{-}pk}(t)$, and is given by:

$$i_{LB1-pk}(t) = \frac{\left|\sqrt{2}v_{AC-rms}\sin(2\pi f_{AC}t)\right|}{2L_{B1}}DT_S \tag{2}$$

where T_S and D are the period and the duty cycle of the power switch, respectively.

When switch S_1 turns off at t_4, this mode finishes.

Mode 5 ($t_4 \leq t < t_5$; in Figure 4e): This mode begins when S_1 is off and i_{LB1} is at its maximum level at t_4. The diode D_{B2} is forward-biased and coupled inductors L_{B1} and L_{B2} provide energy to the drain-source capacitor of S_1 through D_{B2}. The coupled-inductor current i_{LB1} linearly decreases, and it can be given by:

$$i_{LB1}(t) = \frac{V_{DC}}{4L_{B1}}(t - t_4) \tag{3}$$

where V_{DC} represents the voltage of the DC-bus capacitor.

The capacitor C_{DC} and the drain-source capacitor of S_2, provide energy to inductors L_r and L_m and to C_r. The output capacitor C_o continues providing energy to the LED streetlight module. At time interval t_5, the voltage v_{DS2} of power switch S_2 is decreased to zero; then this mode ends.

Mode 6 ($t_5 \leq t < t_6$; in Figure 4f): When the switch voltage v_{DS2} is decreased to zero and the body diode of switch S_2 is forward-biased at t_5, this mode activates and the power switch S_2 turns on with ZVS feature. The voltage source V_{REC2} provides energy to coupled inductor L_{B4} through diode D_{B4} and switch S_2, and the inductor current i_{LB4} increases linearly from zero. The coupled inductors L_{B1} and L_{B2} continue providing energy to the drain-source capacitor of S_1 through D_{B2}, and the inductor current i_{LB1} continues linearly decreasing. The capacitor C_{DC} continues providing energy to inductors L_r and L_m and to the resonant capacitor C_r through the body diode of S_2. The output capacitor C_o continues providing energy to the LED streetlight module. This mode finishes when the magnetizing inductor current i_{Lm} reaches its peak value at t_6.

Mode 7 ($t_6 \leq t < t_7$; in Figure 4g): This mode begins when the magnetizing inductor current i_{Lm} is at its maximum level at t_6. The voltage source V_{REC2} continues providing energy to coupled inductor L_{B4} through diode D_{B4} and switch S_2, and i_{LB4} continues linearly increasing. The coupled inductors L_{B1} and L_{B2} continue providing energy to the drain-source capacitor of S_1 through D_{B2}, and i_{LB1} continues linearly decreasing. The DC-linked capacitor C_{DC} provides energy to the drain-source capacitor of S_1 through S_2. The resonant inductor L_r provides energy to resonant capacitor C_r through switch S_2. The magnetizing inductor L_m provides energy to the output capacitor C_o and the LED streetlight module through transformer T and diode D_2. This mode ends when the inductor current i_{LB1} is decreased to zero at t_7.

Mode 8 ($t_7 \leq t < t_8$; in Figure 4h): This mode activates when the current i_{LB1} is zero at t_7. The voltage source V_{REC2} continues providing energy to coupled inductor L_{B4} through diode D_{B4} and switch S_2. The coupled inductors L_{B1} and L_{B2} continue providing energy to the drain-source capacitor of S_1 through D_{B2}. The DC-linked capacitor C_{DC} continues providing energy to the drain-source capacitor of S_1 through S_2. The resonant inductor L_r and the magnetizing inductor L_m provide energy to resonant capacitor C_r through switch S_2 and to the output capacitor C_o along with the LED streetlight module through transformer T and diode D_2. This mode finishes when the magnetizing inductor current i_{Lm} is decreased to zero at t_8.

Mode 9 ($t_8 \leq t < t_9$; in Figure 4i): This mode begins when the magnetizing inductor current i_{Lm} is zero at t_8. The voltage source V_{REC2} continues providing energy to coupled inductor L_{B4} through diode D_{B4} and switch S_2, and i_{LB4} continues linearly increasing. The DC-linked capacitor C_{DC} continues providing energy to the drain-source capacitor of S_1 through S_2. The inductors L_r and L_m continue providing energy to the capacitor C_r through switch S_2, and to the output capacitor C_o along with the LED streetlight module through transformer T and diode D_2. When the diode current i_{D2} decreases to zero, this mode ends.

Mode 10 ($t_9 \leq t < t_{10}$; in Figure 4j): This mode activates when the current i_{D2} is zero at t_9. The voltage source V_{REC2} continues providing energy to the coupled inductor L_{B4} through D_{B4} and S_2, and i_{LB4} continues increasing linearly. The DC-linked capacitor C_{DC} continues providing energy to the drain-source capacitor of S_1 through S_2. The inductors L_r and L_m continue providing energy to the capacitor C_r through switch S_2. The output capacitor C_o supplies energy to the LED streetlight module. When S_2 turns off and i_{LB4} reaches its peak value at t_{10}, this mode finishes.

Mode 11 ($t_{10} \leq t < t_{11}$; in Figure 4k): This mode begins when switch S_2 is turned off and i_{LB4} is at its maximum level at t_{10}. The coupled inductors L_{B3} and L_{B4} provide energy to the drain-source capacitor of S_2 through D_{B3}, and the inductor current i_{LB4} linearly decreases. The drain-source capacitor of S_1 and the inductors L_r and L_m supply energy to capacitors C_r and C_{DC}. The output capacitor C_o still provides energy to the LED streetlight module. When the switch voltage v_{DS1} decreases to zero at t_{11}, this mode ends, and *Mode 1* begins again for the next switching period.

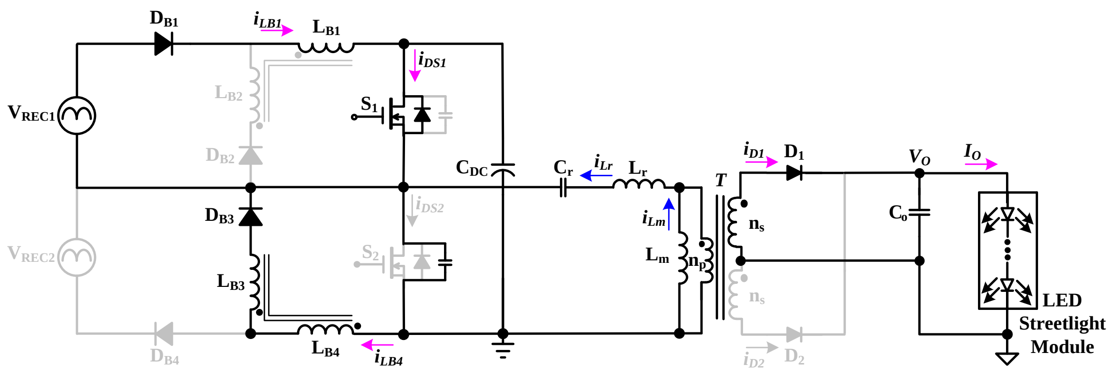

(**a**) *Mode 1* ($t_0 \leq t < t_1$).

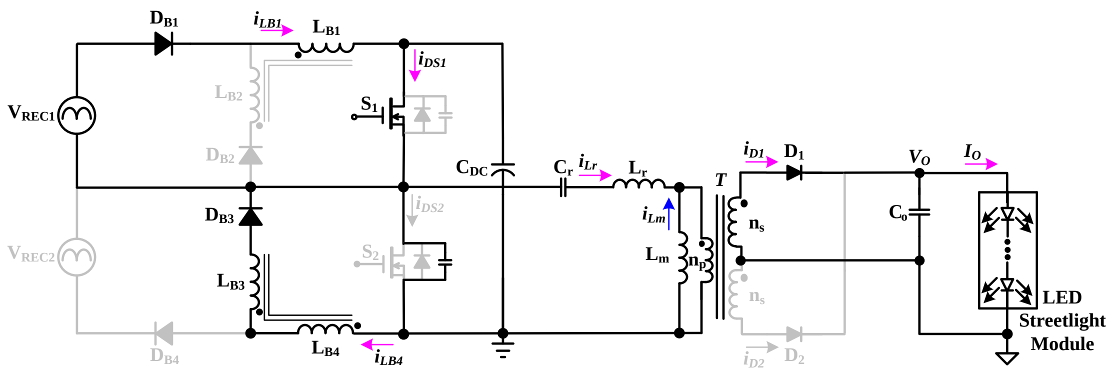

(**b**) *Mode 2* ($t_1 \leq t < t_2$).

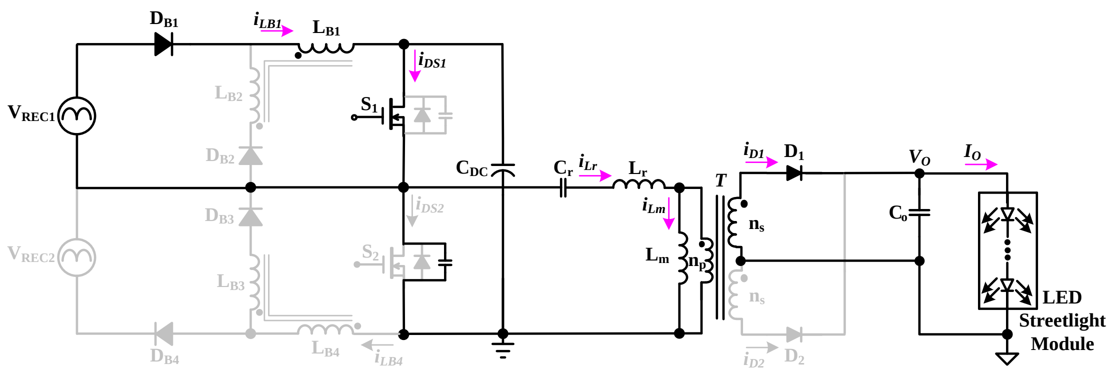

(**c**) *Mode 3* ($t_2 \leq t < t_3$).

Figure 4. *Cont.*

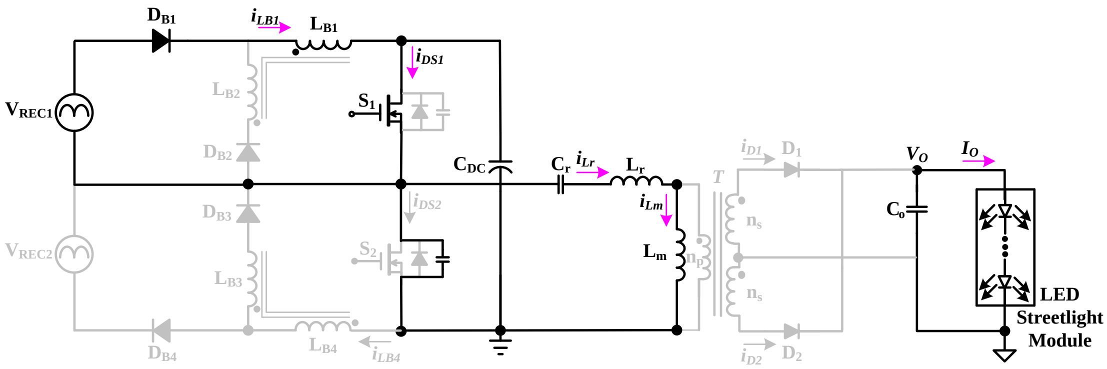

(**d**) *Mode 4* ($t_3 \leq t < t_4$)

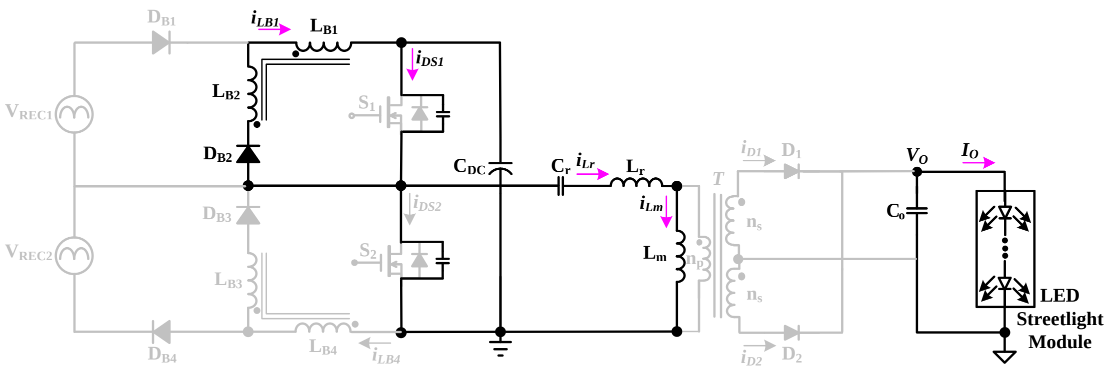

(**e**) *Mode 5* ($t_4 \leq t < t_5$)

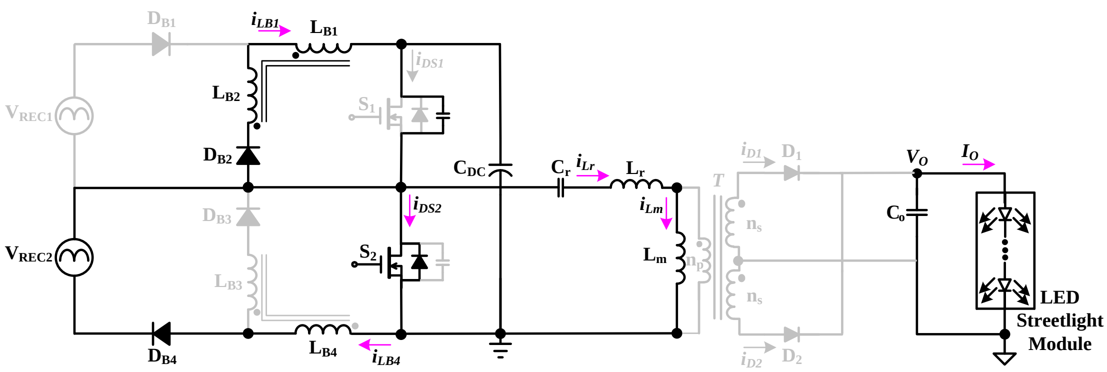

(**f**) *Mode 6* ($t_5 \leq t < t_6$)

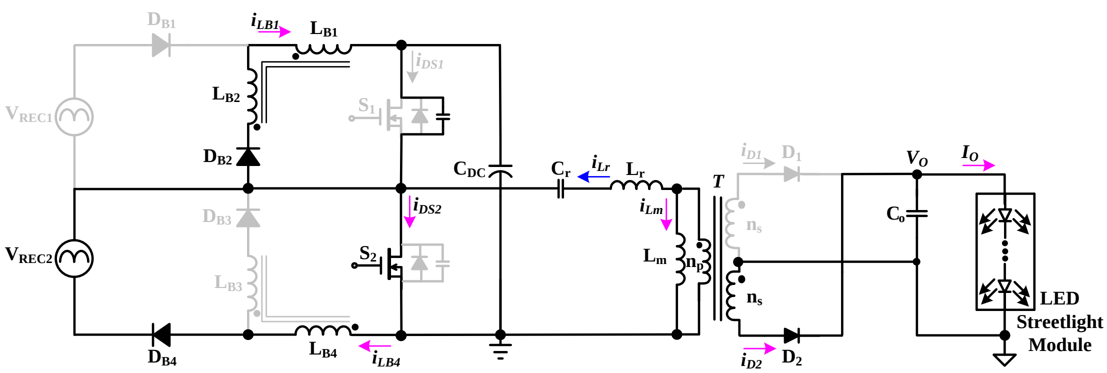

(**g**) *Mode 7* ($t_6 \leq t < t_7$)

Figure 4. *Cont.*

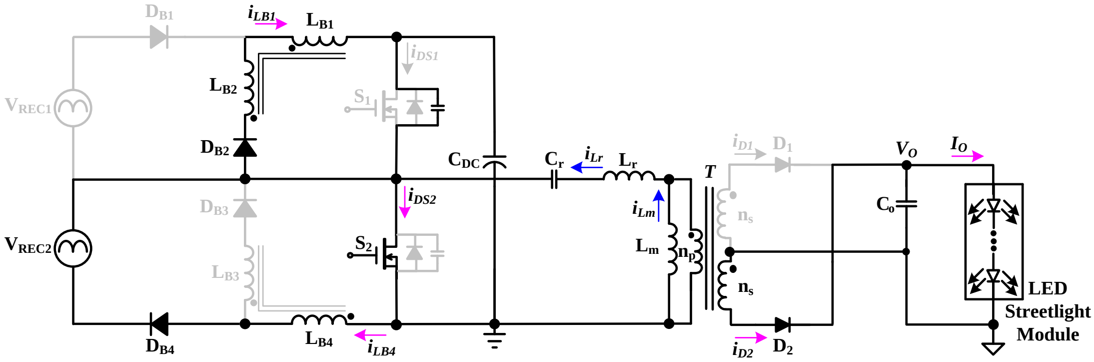

(**h**) *Mode 8* ($t_7 \leq t < t_8$)

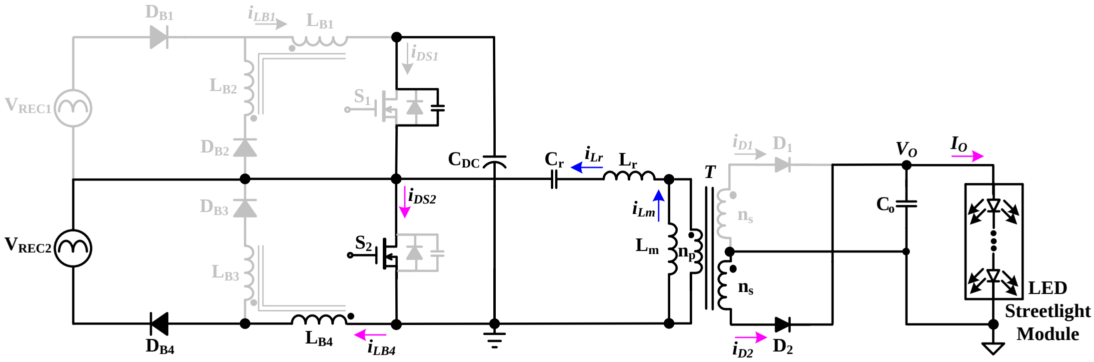

(**i**) *Mode 9* ($t_8 \leq t < t_9$)

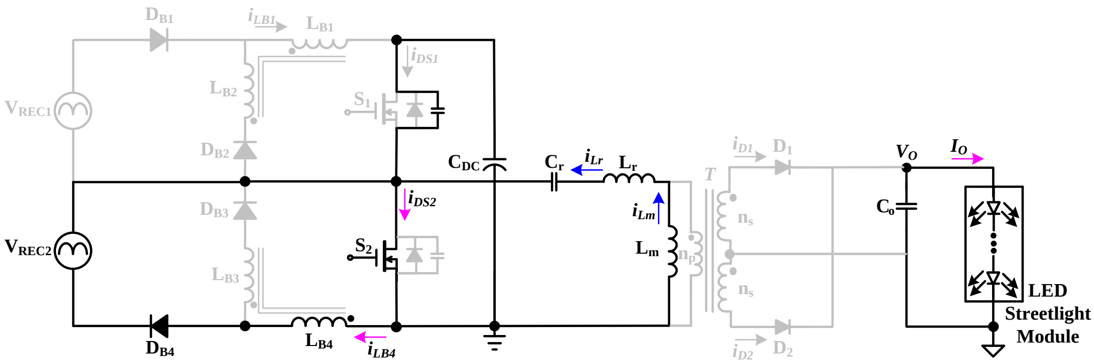

(**j**) *Mode 10* ($t_9 \leq t < t_{10}$)

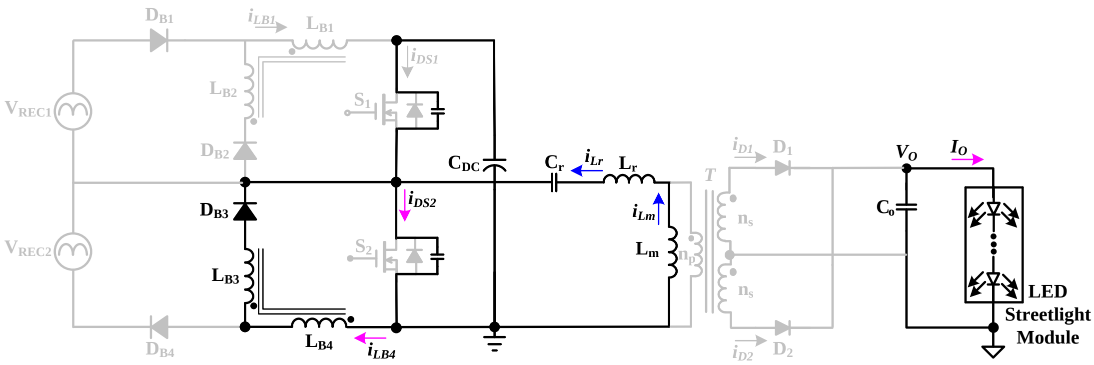

(**k**) *Mode 11* ($t_{10} \leq t < t_{11}$)

Figure 4. Operation modes of the presented LED driver. (**a**) *Mode 1*; (**b**) *Mode 2*; (**c**) *Mode 3*; (**d**) *Mode 4*; (**e**) *Mode 5*; (**f**) *Mode 6*; (**g**) *Mode 7*; (**h**) *Mode 8*; (**i**) *Mode 9*; (**j**) *Mode 10*; (**k**) *Mode 11*.

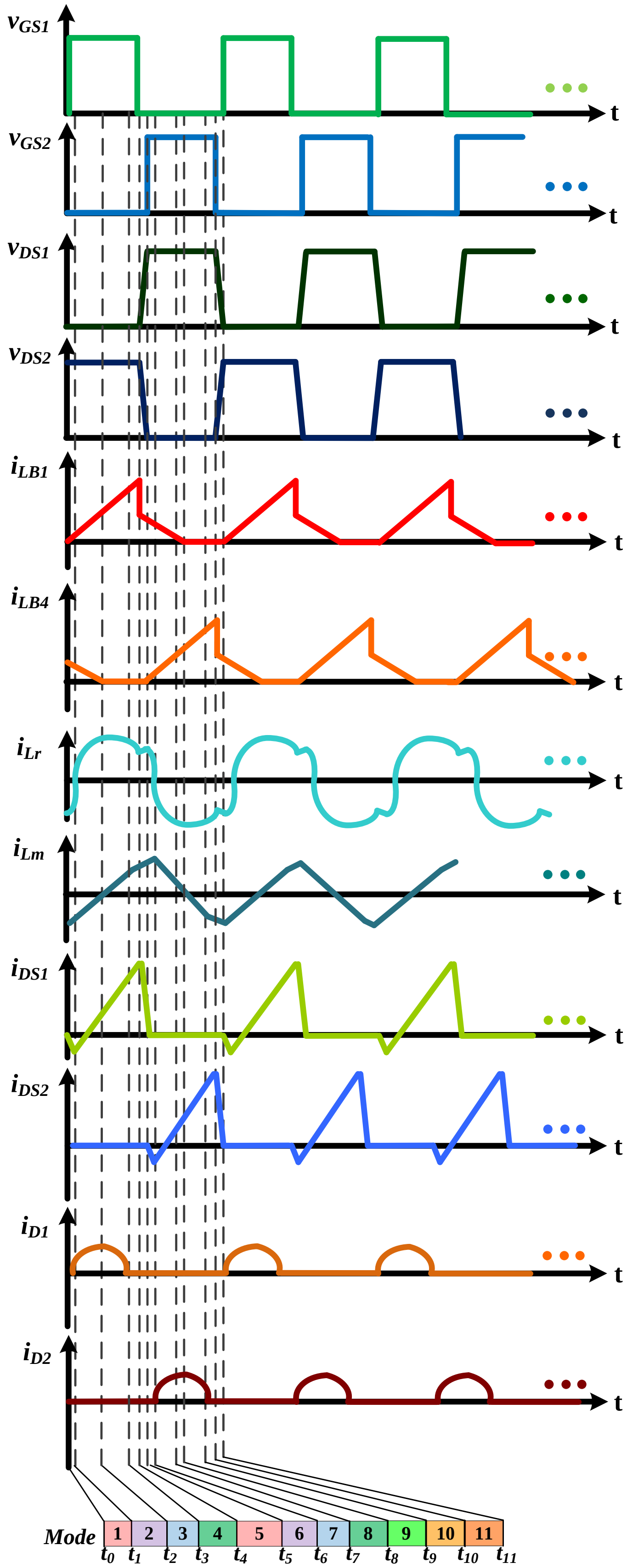

Figure 5. Key waveforms of the presented LED driver for streetlight applications.

3. Design Considerations in the Presented LED Streetlight Driver

3.1. Design of Coupled Inductors L_{B1}, L_{B2}, L_{B3} and L_{B4}

Referring to Figure 3, the rectified voltages V_{REC1} and V_{REC2} are theoretically equal due to the same capacitance of capacitors C_{in1} and C_{in2}, and they can be expressed by

$$V_{REC1}(t) = V_{REC2}(t) = \frac{\sqrt{2}v_{AC-rms}\left|\sin(2\pi f_{AC}t)\right|}{2} \tag{4}$$

The switching frequency f_s is much larger than the line frequency f_{AC}; thus, rectified voltages V_{REC1} and V_{REC2} could be regarded as a constant value during one switching period. Referring to Figure 2b, the peak level of diode currents i_{DB1} and i_{DB4} can be represented by

$$i_{DB1,pk}(t) = i_{DB4,pk}(t) = \frac{\sqrt{2}v_{AC-rms}\left|\sin(2\pi f_{AC}t)\right|Duty}{2L_B f_s} \tag{5}$$

where L_B represents the inductance of coupled inductors L_{B1}, L_{B2}, L_{B3} and L_{B4}, and $Duty$ is the duty cycle of the switches S_1 and S_2.

The peak level of the rectified input current i_{rec}, denoted as $i_{rec,pk}$, can be represented by

$$i_{rec,pk}(t) = i_{DB1,pk}(t) + i_{DB4,pk}(t) = \frac{\sqrt{2}v_{AC-rms}\left|\sin(2\pi f_{AC}t)\right|Duty}{L_B f_s} \tag{6}$$

By filtering the high-frequency components of $i_{rec,pk(t)}$, the input current i_{AC} is equal to the average level of $i_{rec,pk(t)}$ during one switching period and can be expressed as

$$i_{AC}(t) = \frac{1}{T_{AC}}\int_0^{T_{AC}} i_{rec,pk}(t)\cdot dt = \frac{\sqrt{2}v_{AC-rms}Duty^2(\sin(2\pi f_{AC}t))}{2L_B f_s} \tag{7}$$

where T_{AC} is the utility-line period.

The average value of input utility-line power P_{in} is obtained by:

$$P_{in} = \frac{1}{T_{AC}}\int_0^{T_{AC}} v_{AC}(t)i_{AC}(t)dt = \frac{{v_{AC-rms}}^2 Duty^2}{4L_B f_s} \tag{8}$$

The rated output power P_o of the LED street-lighting module is related with input power P_{in} and is given by

$$P_o = \eta P_{in} \tag{9}$$

where η is the estimated efficiency of the LED driver.

From (8) and (9), the design equation of the inductance L_B of coupled inductors is given by

$$L_B = \frac{\eta {v_{AC-rms}}^2 Duty^2}{4P_o f_S} \tag{10}$$

With a η of 0.85, a $Duty$ of 0.5, a P_o of 144 W, a switching frequency f_S of 100 kHz, and a $v_{AC\text{-}rms}$ of 220 V, the inductance L_B of coupled inductors is given by

$$L_B = \frac{0.85\cdot 220^2\cdot 0.5^2}{4\cdot 144\cdot 100k} = 178.6\mu H$$

3.2. Determining the Transformer Turns-Ratio n

The turns-ratio n of transformer T is given as

$$n = \frac{n_p}{n_s} \geq \frac{D\sqrt{2}v_{AC-rms}}{V_o + V_F} \quad (11)$$

where V_F is the forward voltage drop of the output-rectifier diodes D_1 and D_2; and V_o is the output voltage.

With a V_o of 36 V and a V_F of 0.7 V, the turns-ratio n is given by

$$n = \frac{n_p}{n_s} \geq \frac{0.5 \cdot \sqrt{2} \cdot 220}{36 + 0.7} = 4.3$$

The turns-ratio n is selected as 5.

3.3. Determining the LLC Resonant Network

The quality factor Q_r is defined as

$$Q_r = \frac{\sqrt{L_r}}{R_a\sqrt{C_r}} \quad (12)$$

where R_{eq} is the equivalent output resistor referring to the primary side of transformer T, and which can be expressed by the following equation:

$$R_{eq} = \frac{8n^2 V_o}{\pi^2 I_o} \quad (13)$$

The main resonant frequency ω_{r1} and secondary resonant frequency ω_{r2} of the LLC resonant network are respectively defined as

$$\omega_{r1} = 2\pi f_{r1} = \frac{1}{\sqrt{L_r C_r}} \quad (14)$$

$$\omega_{r2} = 2\pi f_{r2} = \frac{1}{\sqrt{(L_m + L_r)C_r}} \quad (15)$$

The inductance ratio A is defined as

$$A = \frac{L_m}{L_r} \quad (16)$$

In addition, substituting (16) into (14) and (15), the secondary resonant frequency f_{r2} is given by

$$f_{r2} = \sqrt{\frac{f_{r1}{}^2}{A+1}} \quad (17)$$

With an f_{r1} of 120 kHz and an A of 5, the secondary resonant frequency f_{r2} is computed by

$$f_{r2} = \sqrt{\frac{(120k)^2}{5+1}} \cong 49kHz$$

Dividing (12) by (14), the resonant inductor L_r can be expressed by

$$L_r = \frac{Q_r R_{eq}}{2\pi f_{r1}} \quad (18)$$

The resonant capacitor C_r can be obtained by

$$C_r = \frac{1}{(2\pi f_{r1})^2 L_r} \tag{19}$$

With an f_{r1} of 120 kHz, an R_{eq} of 182.4Ω, an A of 5 and a Q_r of 0.4, the resonant inductor L_r is given by

$$L_r = \frac{Q_r R_{eq}}{2\pi f_{r1}} = \frac{0.4 \cdot 182.4}{2\pi \cdot 120k} = 96.8\mu H$$

In addition, the inductor L_r is selected as 90 µH, and the magnetic inductor L_m is selected as 450µH according to (16).

The resonant capacitor is given by

$$C_r = \frac{1}{(2\pi f_{r1})^2 L_r} = \frac{1}{(2\pi \cdot 120k)^2 \cdot 90\mu} = 19.5nF$$

Additionally, the resonant capacitor C_r is selected as 22 nF.

3.4. Design Guidelines of Achieving Soft-Switching in the Proposed LED Streetlight Driver

By using the fundamental approximation method, the voltage gain $|M_V|$ of the LLC resonant network is given by [18]:

$$\begin{aligned} \left|M_V(2\pi f_S)\right| &= \frac{n\frac{4V_O}{\pi}\sin 2\pi f_S t}{\frac{2}{\pi}V_{DC}\sin 2\pi f_S t} = \frac{2n \cdot V_o}{V_{DC}} \cong \frac{2n \cdot V_o}{\sqrt{2} \cdot v_{AC-rms}} \\ &= \left|\frac{A\left(\frac{f_S}{f_{r1}}\right)^2}{\left[(A+1)\left(\frac{f_S}{f_{r1}}\right)^2 - 1\right] + jQ_r A\left(\frac{f_S}{f_{r1}}\right)\left[\left(\frac{f_S}{f_{r1}}\right)^2 - 1\right]}\right| \end{aligned} \tag{20}$$

In this design procedure of the proposed LED streetlight driver, the main resonant frequency f_{r1}, the inductance ratio A, and quality factor Q_r are selected to be 120 kHz, 5, and 0.4, respectively. According to (20), Figure 6 shows the relationship between voltage gain $|M_V|$ and switching frequency f_S under different quality factor Q_r. In addition, the right-hand side and left-hand side of the pink line (which is the constraint line for achieving soft-switching) are inductive region and capacitive region, respectively. To achieve soft-switching for reducing power losses in the proposed LED streetlight driver, the LLC resonant network inside the driver is recommended to be operated at inductive region. Moreover, with a turns-ratio n of 5, an output voltage V_O of 36V and a rated input utility-line voltage $v_{AC\text{-}rms}$ of 220V, the rated voltage gain $M_{V\text{-}rated}$ is obtained by

$$M_{V-rated} = \frac{2nV_O}{\sqrt{2} \cdot v_{AC-rms}} = \frac{2 \cdot 5 \cdot 36}{\sqrt{2} \cdot 220} = 1.16$$

In addition, the switching frequency f_S is designed at 100 kHz under a rated voltage gain $M_{V\text{-}rated}$ of 1.16. If the rated input utility-line voltage has some variations (for example, 10V), the required maximum voltage gain $M_{V\text{-}max}$ occurred at minimum input voltage and the required minimum voltage gain $M_{V\text{-}min}$ occurred at maximum input voltage are respectively calculated by

$$M_{V-\max} = \frac{2nV_O}{\sqrt{2} \cdot v_{AC-\min}} = \frac{2 \cdot 5 \cdot 36}{\sqrt{2} \cdot (220 - 10)} = 1.21$$

$$M_{V-\min} = \frac{2nV_O}{\sqrt{2} \cdot v_{AC-\max}} = \frac{2 \cdot 5 \cdot 36}{\sqrt{2} \cdot (220 + 10)} = 1.11$$

Please see Figure 6, by using variable frequency control scheme, the switching frequencies under required maximum and minimum voltage gains ($M_{V\text{-}max}$ and $M_{V\text{-}min}$) are adjusted to be 90 kHz and 110 kHz due to variations of input utility-line voltage, respectively. Furthermore, these switching frequencies are located at the right-hand side of the pink line. As a result, soft-switching features are also achieved when the rated input utility-line voltage has variations of 10 V.

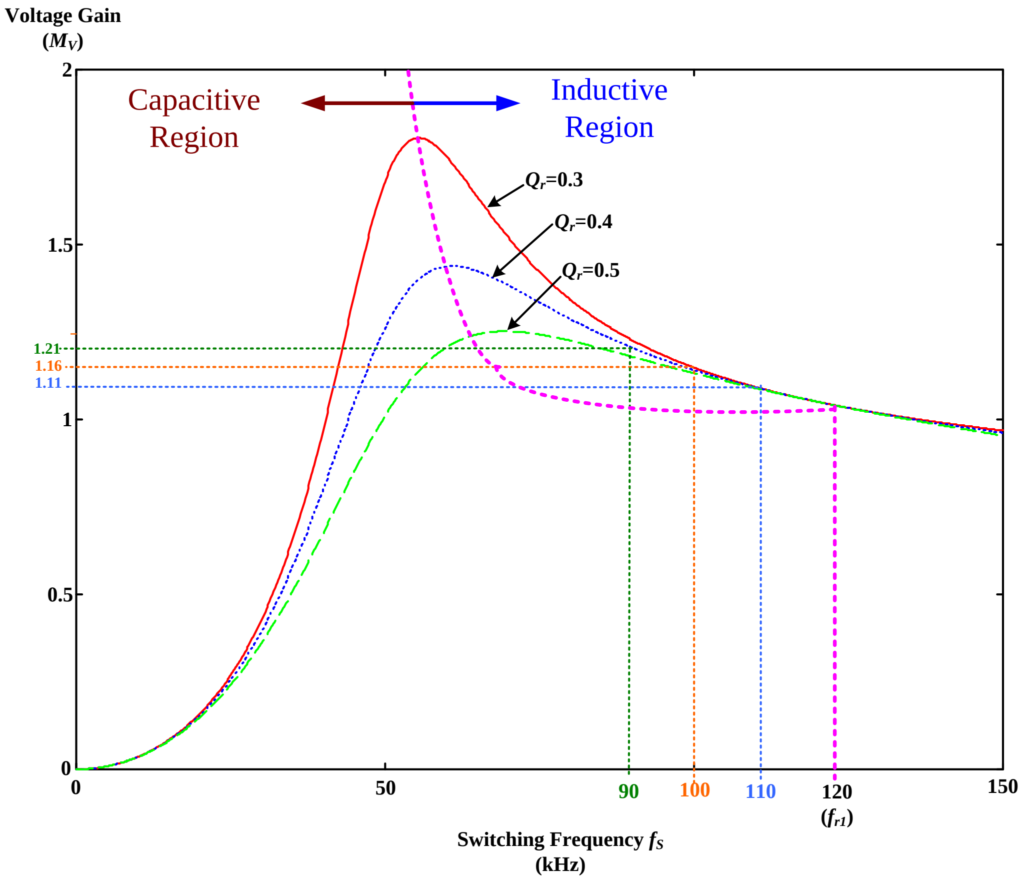

Figure 6. Relationship between the voltage gain M_V of LLC resonant tank and the switching frequency f_S.

4. Experimental Results of the Prototype LED Streetlight Driver

A prototype driver has been successfully developed and implemented for supplying a 144 W-rated (36V/4A) LED streetlight module with an input utility-line voltage of 220 V. Tables 1 and 2, respectively, show the specifications and key components utilized in the presented single-stage LED streetlight driver. Additionally, Figure 7 shows the proposed LED streetlight driver with control block diagram. A constant-voltage and constant-current (CV-CC) controller is adopted to sense the output voltage through resistors R_{VS1} and R_{VS2}, while simultaneously sensing the output current through the resistor R_{CS} for supplying the rated voltage and current to the experimental LED street-lighting module. The output signal of the CV-CC controller feeds into the high-voltage resonant controller through a photo-coupler. Two gate-driving signals v_{gs1} and v_{gs2} generating from the resonant controller regulate the output voltage and current of the LED street-lighting module by utilizing variable-frequency control scheme. Moreover, the coupled-inductors (L_{B1}, L_{B2}, L_{B3} and L_{B4}) are designed to be operated at discontinuous conduction mode (DCM) for naturally achieving input-current shaping without utilizing a power-factor-correction controller with a feed-forward controlling path.

Table 1. Specifications of the presented singles-stage LED streetlight driver.

Parameter	Value
Input Utility-Line Voltage v_{AC}	220 V (rms)
Output Rated Power P_O	144 W
Output Rated Voltage V_O	36 V
Output Rated Current I_O	4 A

Table 2. Key components utilized in the presented LED streetlight driver.

Component	Value
Capacitors C_{in1}, C_{in2}	330 nF
Inductors L_{B1}, L_{B2}, L_{B3}, L_{B4}	179 µH
Diodes D_{B1}, D_{B2}, D_{B3}, D_{B4}	MUR460
Power Switches S_1, S_2	STP20NM60
DC-Linked Capacitor C_{DC}	220 µF/450 V
Magnetizing Inductor L_m	450 µH
Resonant Inductor L_r	90 µH
Resonant Capacitor C_r	22 nF
Diodes D_1, D_2	MBR30H100CT
Output Capacitor C_o	2200 µF/63 V
Filter Inductor L_f	2.5 mH
Filter Capacitor C_f	1 µF

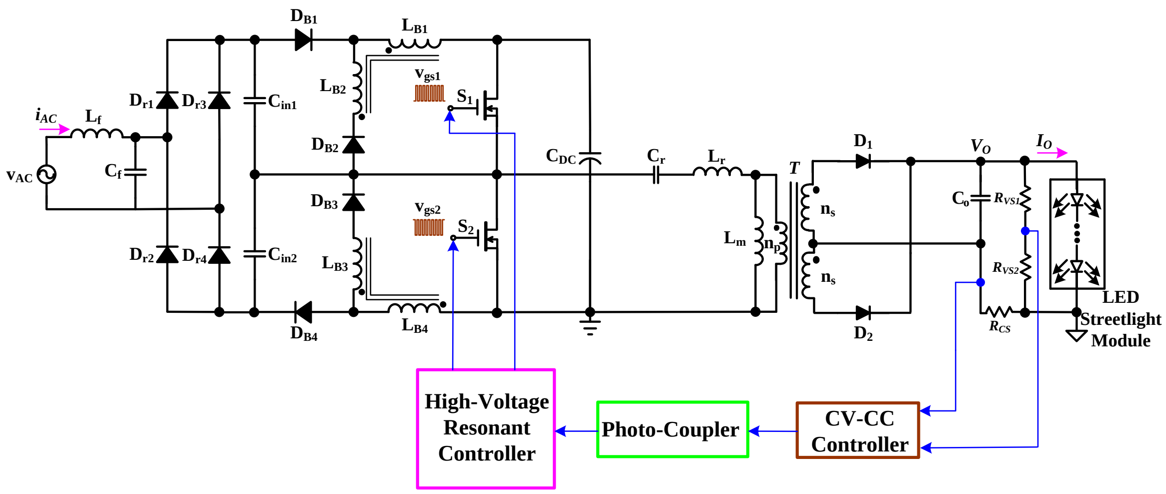

Figure 7. The proposed LED streetlight driver with control block diagram.

The measured waveforms of coupled-inductor currents i_{LB1} and i_{LB4} are shown in Figure 8; both have interleaved features and operate in DCM. Figure 9 shows the measured switch voltage v_{DS2} and switch current i_{DS2}; thus, ZVS has occurred on the power switch for lowering switching losses. Figure 10 presents the measured switch voltage v_{DS2} and resonant inductor current i_{Lr}. Figure 11 presents the measured switch voltage v_{DS2} and current i_{D2} of the output rectified diode D_2; thus, ZCS has occurred on the power diode for decreasing the conduction losses. Figure 12 depicts the measured output voltage V_O and current I_O; their average values are approximately 36 V and 4 A, respectively.

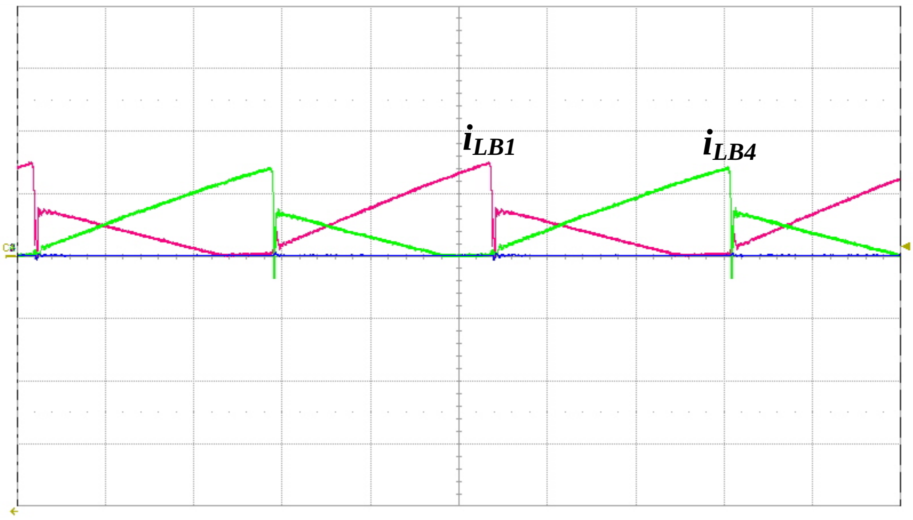

Figure 8. Measured currents i_{LB1} (2 A/div) and i_{LB4} (2 A/div) of the coupled inductors; time scale: 2 µs/div.

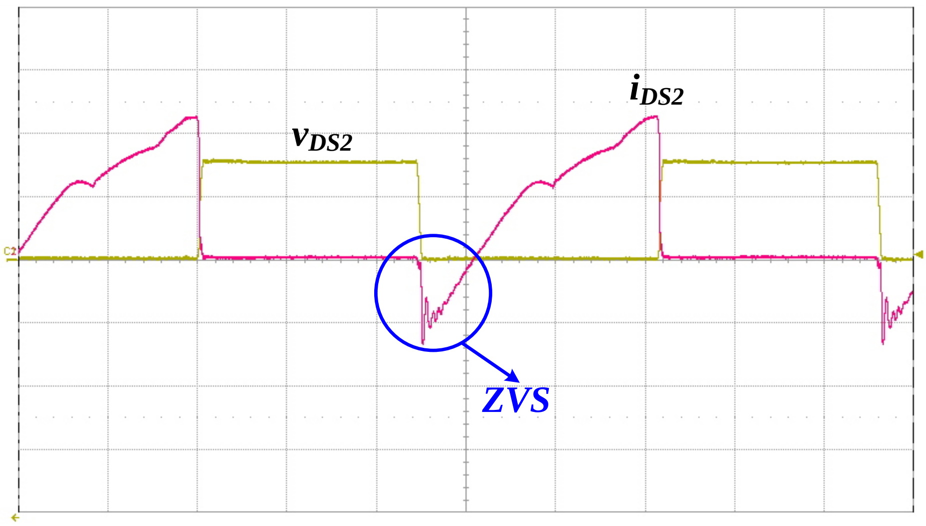

Figure 9. Measured switch voltage v_{DS2} (200 V/div) and current i_{DS2} (2 A/div); time scale: 2 µs/div.

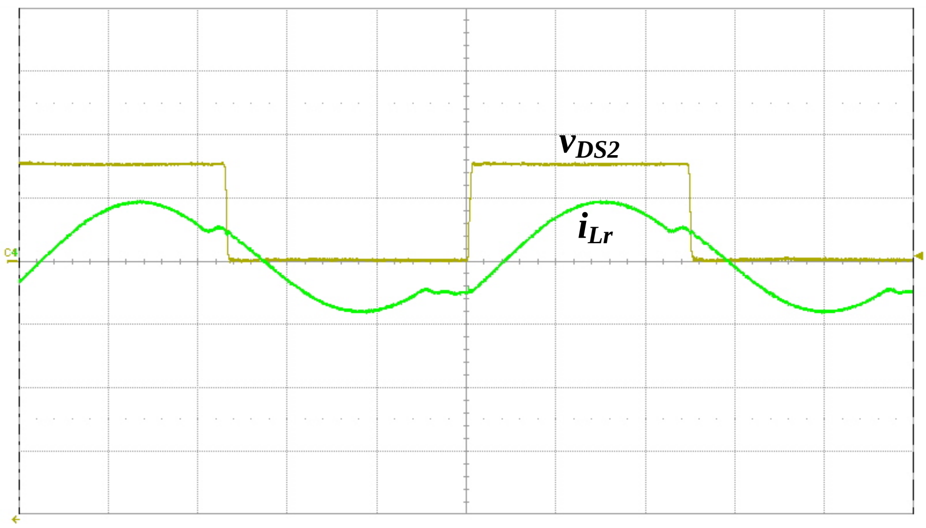

Figure 10. Measured switch voltage v_{DS2} (200 V/div) and current i_{Lr} (2 A/div); time scale: 2 µs/div.

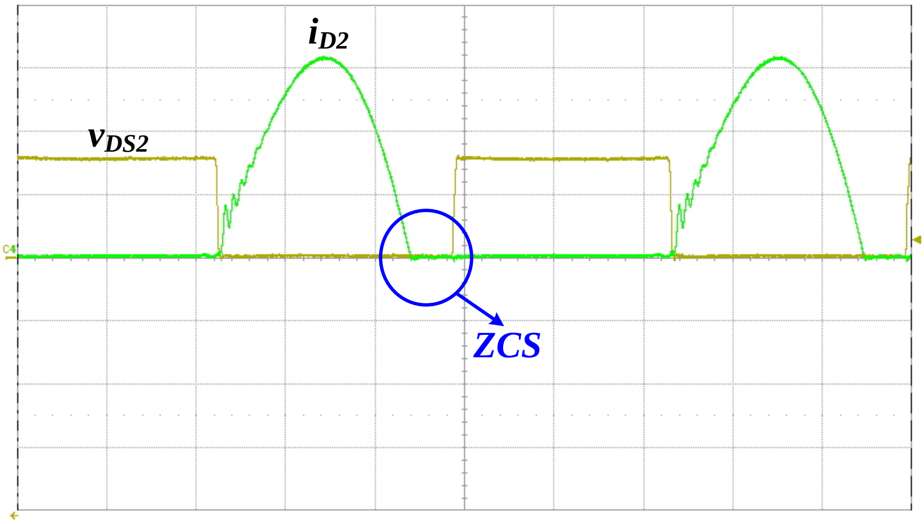

Figure 11. Measured switch voltage v_{DS2} (200 V/div) and current i_{D2} (2 A/div) of the output rectified diode D_4; time scale: 2 μs/div.

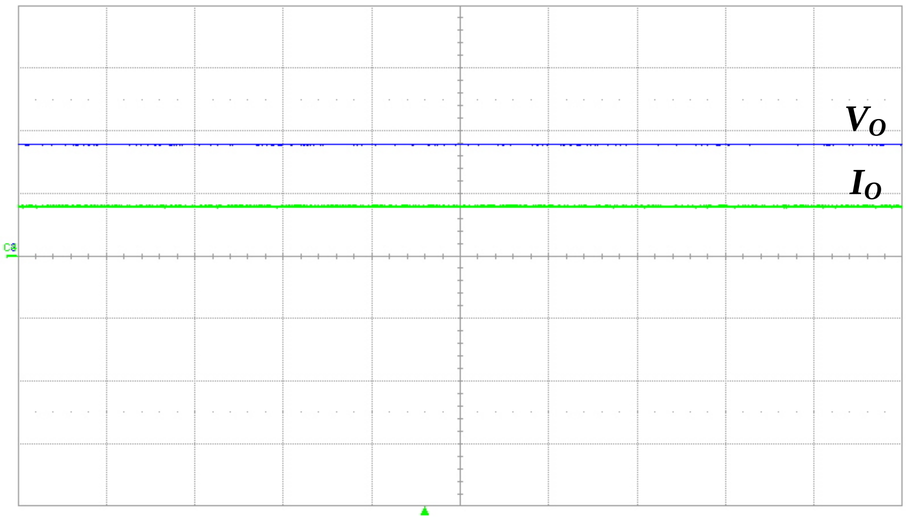

Figure 12. Measured output voltage V_O (20 V/div) and current I_O (5 A/div); time scale: 5ms /div.

The measured waveforms of input utility-line voltage v_{AC} and current i_{AC} are shown in Figure 13, and the input current is in phase with utility-line voltage, which results in high power factor. In addition, the measured power factor and the circuit efficiency are 0.9684 and 89.69%, respectively, as measured by a power analyzer (Tektronix PA 4000). Figure 14 shows the measured input utility-line current harmonics at an input utility-line voltage of 220 V in comparison with the International Electrotechnical Commission (IEC) 61000-3-2 Class C standards; all utility-line current harmonics meet the requirements.

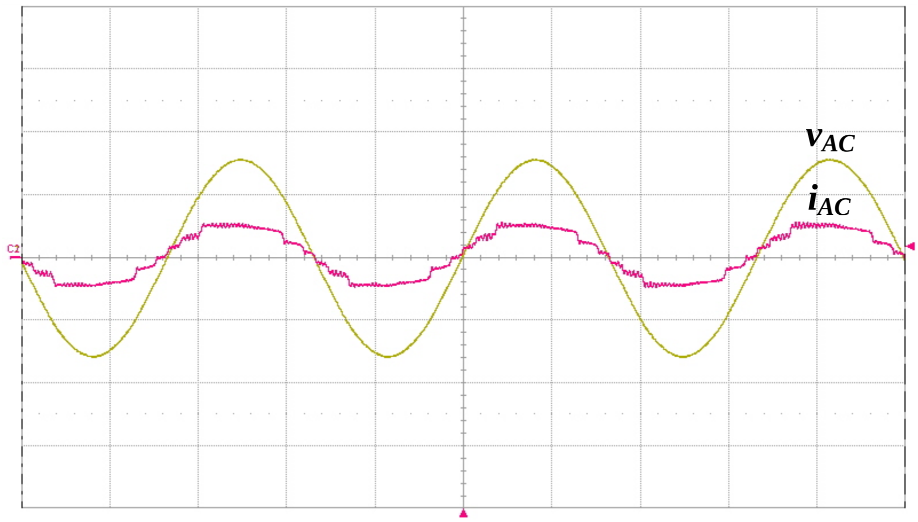

Figure 13. Measured input utility-line voltage v_{AC} (200 V/div) and current i_{AC} (2 A/div); time scale: 5 ms/div.

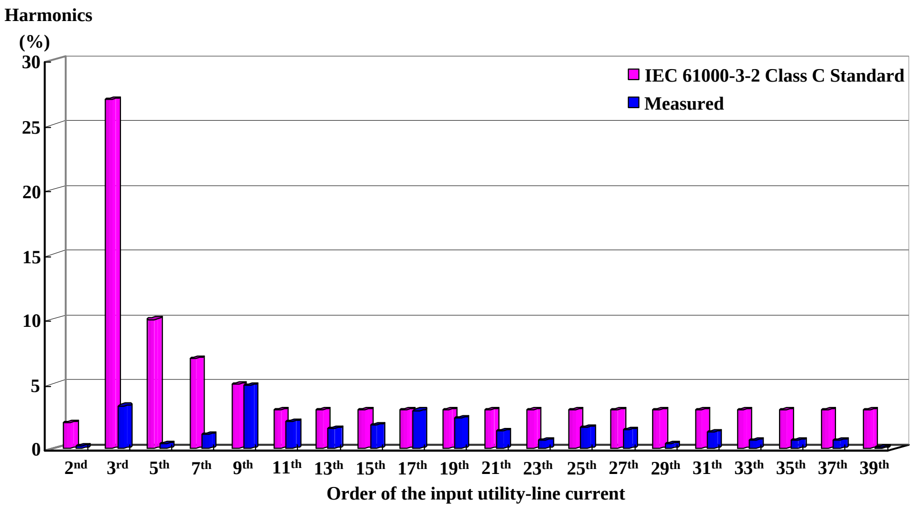

Figure 14. Measured input current harmonics compared with the IEC 61000-3-2 Class C standards.

Table 3 shows the measured output voltage ripple and current ripple of the presented LED streetlight driver at a utility-line voltage of 220 V; additionally, the output voltage (current) ripple factor is obtained by the peak-to-peak level divided by the mean value of output voltage (current). It can be seen that the measured voltage and current ripple factors are smaller than 5% and 2%, respectively. Figure 15 presents a photo of supplying the LED streetlight module with the proposed streetlight driver at an input utility-line voltage of 220V. In addition, Table 4 shows comparisons between the existing single-stage LED streetlight driver in references [16–19] and the one proposed in this paper. According to this table, the proposed single-stage LED streetlight driver has a beneficial feature of reduced voltage stress of power switches, which is favorable for operating with high utility-line voltages, in comparison to the existing single-stage versions in the references [16–19]. In addition, the proposed circuit has the lowest current ripple factor among these LED streetlight drivers.

Table 3. Measured output voltage ripple and current ripple of the presented LED streetlight driver at a utility line voltage of 220V.

Parameter	Value
Mean Value of Output Voltage V_O	35.85 V
Peak-to-Peak Value of Output Voltage V_O	1.53 V
Voltage Ripple Factor	4.28 %
Mean Value of Output Current I_O	3.95 A
Peak-to-Peak Value of Output Current I_O	48.9 mA
Current Ripple Factor	1.24 %

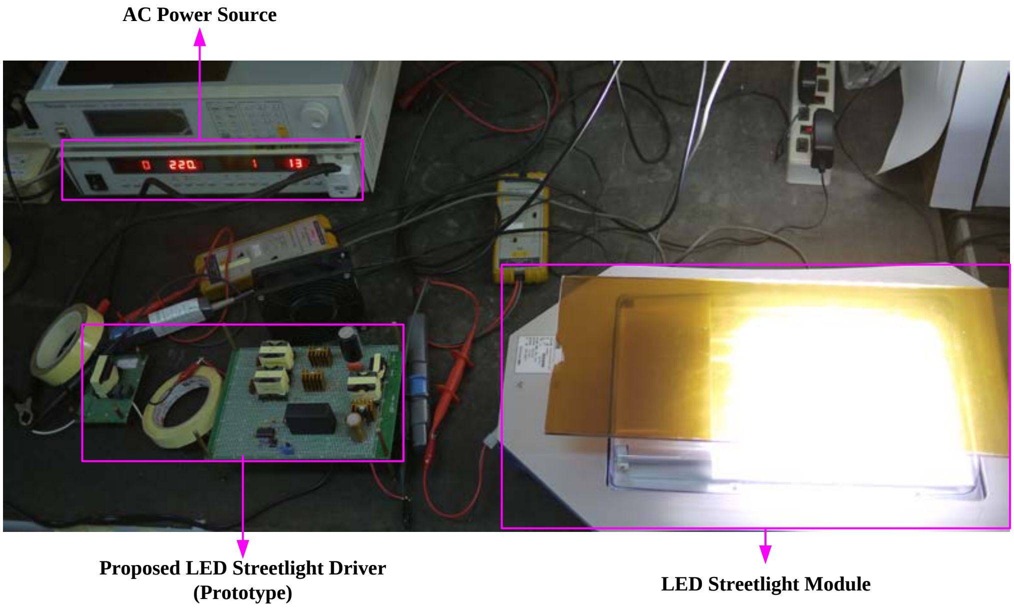

Figure 15. Photo of supplying the LED streetlight module with the proposed streetlight driver at a input utility-line voltage of 220V.

Table 4. Comparisons between the existing single-stage LED streetlight driver in [16–19], and the version proposed in this paper.

Item	Presented Driver in Reference [16]	Presented Driver in Reference [17]	Presented Driver in Reference [18]	Presented Driver in Reference [19]	Proposed Driver
Circuit Topology	Integration of interleaved boost PFC converter and LLC resonant converter	Integration of dual buck-boost converter with coupled inductors and LLC resonant converter	Integration of modified bridgeless boost PFC converter and LLC resonant converter	Integration of dual boost converter with coupled inductors and LLC resonant converter	Integration of interleaved buck-boost converter with coupled inductors and LLC resonant converter
Number of Required Power Switches	2	2	2	2	2
Number of Required Diodes	8	6	4	4	10
Number of Required Capacitors	6 (Including one DC-bus capacitor)	5 (Including two DC-bus capacitors)	4 (Including one DC-bus capacitor)	4 (Including one DC-bus capacitor)	6 (Including one DC-bus capacitor)
Number of Required Magnetic Components	5	4	4	4	5
Input Utility-Line Voltage	110V	110V	110V	110V	220V
Output Power	144W (36V/4A)	144W (36V/4A)	144W (36V/4A)	144W (36V/4A)	144W (36V/4A)
Voltage Stress of Power Switches	$\frac{1}{1-D}\sqrt{2}v_{AC-rms}$	$\frac{2D}{1-D}\sqrt{2}v_{AC-rms}$	$\frac{1}{1-D}\sqrt{2}v_{AC-rms}$	$\frac{1}{1-D}\sqrt{2}v_{AC-rms}$	$\frac{D}{1-D}\sqrt{2}v_{AC-rms}$
Voltage Ripple Factor	< 6%	< 7%	< 8%	< 4%	< 5%
Current Ripple Factor	< 10%	< 5%	< 13%	< 4%	< 2%
Measured Power Factor	> 0.99	> 0.99	> 0.99	> 0.98	> 0.97
Measured Circuit Efficiency	> 88 %	> 90%	> 92%	> 92%	≒ 90%

5. Conclusions

This paper has presented and implemented a single-stage LED streetlight driver with soft-switching and PFC features; the proposed circuit integrates an interleaved buck-boost converter with coupled inductors and a half-bridge LLC resonant converter into a single power-conversion stage, and is suitable for operating at high utility-line voltages with reduced voltage stress on the DC-linked capacitor. A 144 W prototype LED driver has been developed and tested with an input utility-line voltage of 220 V. The experimental results of the presented LED streetlight driver display low output-voltage ripple factor (< 5%), low output-current ripple factor (< 2%), high power factor (> 0.97), ZVS on power switches, ZCS on output rectified diodes, and high circuit efficiency (approximately 90%); thus the functionality of the presented LED streetlight driver is validated.

Author Contributions: C.-A.C. and C.-H.C. conceived and designed the circuit. H.-L.C. and E.-C.C. performed circuit simulations. T.-Y.C. and M.-T.C. carried out the prototype driver, and measured as well as analyzed experimental results with the guidance from C.-A.C. E.-C.C. revised the manuscript for submission.

Funding: This research was funded by the Ministry of Science and Technology (MOST) of Taiwan, R.O.C., under its grant with reference number MOST 105-2221-E-214-028.

Acknowledgments: The authors would like to convey their appreciation for grant support from the Ministry of Science and Technology (MOST) of Taiwan, R.O.C., under its grant with reference number MOST 105-2221-E-214-028.

Conflicts of Interest: The authors declare no conflict of interest.

References

1. Schubert, E.F. *Light-Emitting Diodes*; Cambridge University Press: New York, NY, USA, 2006.
2. Bender, V.C.; Marchesan, T.B.; Alonso, J.M. Solid-state lighting: A concise review of the state of the art on LED and OLED modeling. *IEEE Ind. Electron. Mag.* **2015**, *9*, 6–16. [CrossRef]
3. Almeida, P.S.; Camponogara, D.; Braga, H.; Dalla Costa, M.A.; Alonso, J.M. Matching LED and driver life spans: A review of different techniques. *IEEE Ind. Electron. Mag.* **2015**, *9*, 36–47. [CrossRef]
4. Liang, T.J.; Tseng, W.J.; Chen, J.F.; Wu, J.P. A novel line frequency multistage conduction LED driver with high power factor. *IEEE Trans. Power Electron.* **2015**, *30*, 5103–5115. [CrossRef]
5. Lee, S.W.; Choe, H.J.; Yun, J.J. Performance improvement of a boost LED driver with high voltage gain for edge-lit LED backlights. *IEEE Trans. Circuits Syst. II Express Briefs* **2018**, *65*, 481–485. [CrossRef]
6. Kuo, T.H.; Liang, T.J.; Wu, W.J. Design and implementation of a LED driver with current balancing. In Proceedings of the IEEE 8th International Power Electronics and Motion Control Conference (IPEM-ECCE Asia), Hefei, China, 22–26 May 2016; pp. 3306–3313.
7. Cheng, H.L.; Lin, C.W. Design and implementation of a high power-factor LED driver with zero-voltage switching-on characteristics. *IEEE Trans. Power Electron.* **2014**, *29*, 4949–4958. [CrossRef]
8. Wang, Y.; Zhang, S.; Alonso, J.M.; Liu, X.; Xu, D. A single-stage LED driver with high-performance primary-side-regulated characteristic. *IEEE Trans. Circuits Syst. II Express Briefs* **2018**, *65*, 76–80. [CrossRef]
9. Alonso, J.M.; Perdigão, M.S.; Abdelmessih, G.Z.; Dalla Costa, M.A.; Wang, Y. SPICE modeling of variable inductors and its application to single inductor LED driver design. *IEEE Trans. Ind. Electron.* **2017**, *64*, 5894–5903. [CrossRef]
10. Wang, Y.; Guan, Y.; Xu, D.; Wang, W. A CLCL resonant DC/DC converter for two-stage LED driver system. *IEEE Trans. Ind. Electron.* **2016**, *63*, 2883–2891. [CrossRef]
11. Luo, Q.; Huang, J.; He, Q.; Ma, K.; Zhou, L. Analysis and design of a single-stage isolated AC-DC LED driver with a voltage doubler rectifier. *IEEE Trans. Ind. Electron.* **2017**, *64*, 5807–5817. [CrossRef]
12. Camponogara, D.; Ferreira, G.F.; Campos, A.; Dalla Costa, M.A.; Garcia, J. Offline LED driver for street lighting with an optimized cascade structure. *IEEE Trans. Ind. Appl.* **2013**, *49*, 2437–2443. [CrossRef]
13. Arias, M.; Lamar, D.G.; Sebastian, J.; Balocco, D.; Diallo, A. High-efficiency LED driver without electrolytic capacitor for street lighting. *IEEE Trans. Ind. Appl.* **2013**, *49*, 127–137. [CrossRef]
14. Arias, M.; Lamar, D.G.; Linera, F.F.; Balocco, D.; Diallo, A.A.; Sebastian, J. Design of a soft-switching asymmetrical half-bridge converter as second stage of an LED driver for street lighting application. *IEEE Trans. Power Electron.* **2012**, *27*, 1608–1621. [CrossRef]

15. Wang, Y.; Guan, Y.; Liang, X.; Wang, W.; Xu, D. Two-stage LED street lighting system based on a novel single-stage AC/DC converter. *IET Power Electron.* **2014**, *7*, 1374–1383. [CrossRef]
16. Cheng, C.A.; Cheng, H.L.; Chang, C.H.; Yang, F.L.; Chung, T.Y. A single-stage LED driver for street-lighting applications with interleaving PFC feature. In Proceedings of the IEEE 2nd International Symposium on Next-Generation Electronics, Kaohsiung, Taiwan, 25–26 February 2013; pp. 150–152.
17. Cheng, C.A.; Cheng, H.L.; Chung, T.Y. A novel single-stage high-power-factor LED street-lighting driver with coupled inductors. *IEEE Trans. Ind. Appl.* **2014**, *50*, 3037–3045. [CrossRef]
18. Cheng, C.A.; Chang, C.H.; Chung, T.Y.; Yang, F.L. Design and implementation of a single-stage driver for supplying an LED street-lighting module with power factor corrections. *IEEE Trans. Power Electron.* **2015**, *30*, 956–966. [CrossRef]
19. Cheng, C.A.; Chung, T.Y. A single-stage LED streetlight driver with PFC and digital-PWM-dimming capability. *Int. J. Circuit Theory Appl.* **2016**, *44*, 1942–1958. [CrossRef]
20. Cheng, C.A.; Tseng, C.H.; Feng, P.H.; Tseng, K.C. A novel single-stage LED driver for energy-saving streetlight applications with interleaved power-factorcorrection. *Int. J. Green Energy* **2018**, *15*, 286–295. [CrossRef]